RSC Advances

ROYAL SOCIETY OF CHEMISTRY

www.rsc.org/advances

Cite this: DOI: 10.1039/c0xx00000x

www.rsc.org/xxxxxx

ARTICLE TYPE

A smart and rapid colorimetric method for detection of codeine sulphate, using unmodified gold nanoprobe

Anand Lodha[a], Alok Pandya[b], Pinkesh Sutariya[c] and Shobhana K. Menon[ac]*

Driven by need to detect narcotics, we designed a "smart" system for rapid detection and quantification of codeine sulphate levels using a smartphone, which allows simple, portable, on-spot, rapid, ultrasensitive nano aggregation colorimetric detection (lower detection limit 0.9 µM) using the unique properties of citrate stabilized gold nanoparticles (AuNPs) as a probe.

The number of drug-facilitated crimes seems to have increased during the last few years. Detecting drugs of abuse have become a challenge to many forensic scientists because of its less availability in the pristine form in the sample which is sent for examination. Another challenge for scientists is to detect the drug in trace amounts of biological specimens. Forensic scientist receives different types of biological samples like blood, saliva, semen, urine etc. from scene of crime[1]. It is very difficult to analyze unidentified, putrefied or skeletonised human remains to obtain information on drug habits, which may prove important for the construction of a biological profile or lead to hypotheses on the manner of death. Bone and bone marrow are specimens recently investigated for drug testing and the drug finding in bone and bone marrow has very high relevance in forensic investigation[2]. In some cases, forensic analysis of skeletal remains may provide the precious information of the deceased. The presence of abusive drug is traditionally not examined in bone, bone marrow and soil samples. The new approach adopted in this investigation will provide new direction that may not have otherwise existed. There is a paucity of basic research on drug deposition in human skeletal remains, which virtually debar the ability to associate a measured drug concentration in a bone or bone marrow sample in forensic investigation[2(g)].

Currently, many different techniques exist for detection of the drugs and its metabolites from different types of samples. The most common techniques, which are routinely in use, are high performance liquid chromatography[3], absorption spectroscopy[4], IR spectroscopy[5], thin layer chromatography[6], mass spectrometry (MS) and gas chromatography (GC)[7]. However, these methods require sophisticated equipment, which are quite inconvenient for outdoor detection or for on-spot analysis. Hence, it is necessary to develop a simple, cost effective, highly sensitive and smart techniques for the detection of drugs of forensic interest.

In recent years, gold nanoparticles (AuNPs) have drawn much attention owing to their excellent biocompatibility, unique optical and electrochemical properties[8] and their applications to the sensing of various analytes including proteins, DNA, amino acids and metal ions with a sensing mechanism, based on analyte induced changes in their absorption and fluorescence, which are widely researched[9]. Recently these unique optical properties are smartly utilized in quantitative analysis using the digital imaging and smartphone cameras. Measurement of shades of colorimetric product in digital image facilitates a quantitative analysis using the color space and imaging devices[10]. Recently, we reported a novel nanoaggregation detection technique of TNT using nano curcumin as a probe[11], potassium ion recognition by benzo-15-crown-5-gold nanoparticles[12], selective amino acid recognition of lysine, arginine and histidine by functionalized calix [4] arene thiol AuNPs[13], "on-spot" colorimetric recognition of clonazepam by melamine modified AuNP[14] and rapid colorimetric detection of sulfide using calix [4] arene modified AuNPs as a probe[15]. The sensitivity and selectivity of these sensors prompted us to design and develop sensors on the same line for codeine sulphate.

The surface adsorption of electron-rich ligands on AuNPs has been well recognized in the literature[16]. Hydroxyl groups with electron-rich oxygen atoms are more likely to be bound onto the surface of metal nanoparticles through the coordinating interactions with the electron-deficient surface of metal nanoparticles[17]. In particular, oxygen containing ring of hybrid aromatics exhibit much stronger binding to AuNPs and therefore the furan like compounds are often used as transfer agents of AuNPs from one phase to another or as a mediator of aggregating state of metal nanoparticles. Accordingly, codeine sulphate with multiple binding sites containing sulphate groups and an oxygen hybrid ring may strongly co-ordinate to AuNPs by the ligand exchange with weakly surface-bound citrate ions, and finally cross-link AuNPs. The colloidal stability is significantly reduced to result in the prompt occurrence of particle aggregation, as revealed in **Fig. 1A**. The molecular linker-based aggregation offers a new approach to a simple and rapid colorimetric assay for the detection of codeine sulphate in bone, bone marrow and soil, which does not require any extra aid such as specific acceptors.

The AuNPs synthesis procedure was essentially the same as that developed by Menon et al[15] (**ESI**). 1 mL of codeine sulphate was added into 2 mL of the AuNPs (0.07 mM) suspension in phosphate buffer (pH 7.5). The shift in the surface plasmon resonance (SPR) absorption maxima of the AuNPs on adding predetermined quantities of codeine sulphate standard was recorded using a UV-Visible absorption spectrophotometer and the same resultant color product were photographed with iPhone 5S in a safety cabinet for smart analysis. The aggregating kinetics of AuNPs with 1 µM to 1 mM codeine sulphate was obtained by

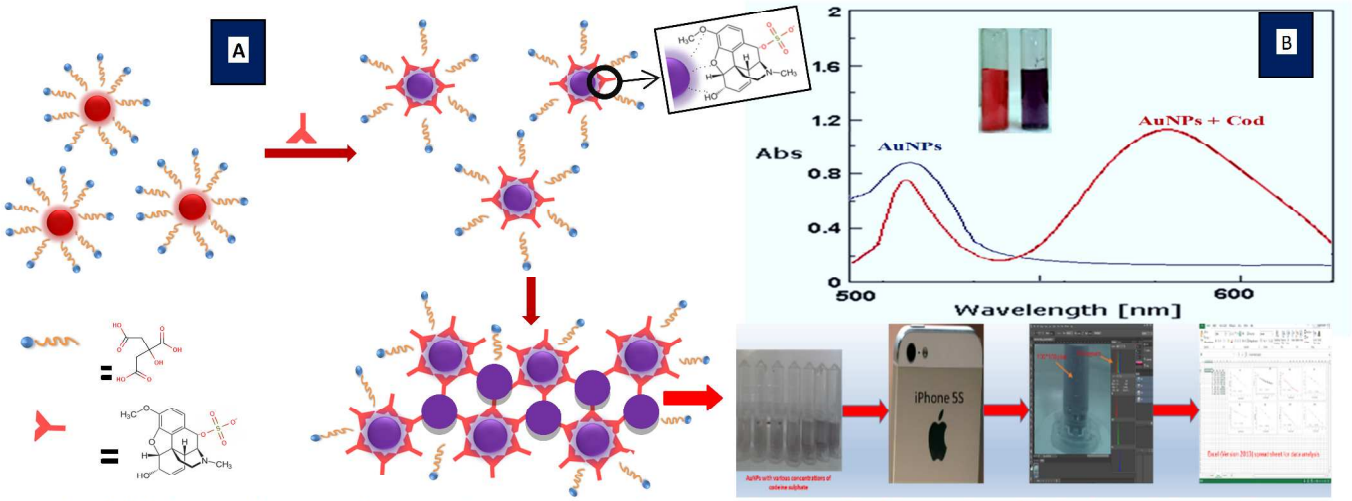

Fig. 1 (A) Schematic illustration of interaction between codeine sulphate and citrate caped AuNPs and its resultant color products smartphone analysis **(B)** Absorption spectral changes of citrate stabilized AuNPs in the presence of 10 µM codeine sulphate

measuring the absorbance and intensity of the red, green, blue light and total RGB at an interval of 2 min and these were further optimized. The calibration curve were plotted with the wavelength against the absorbance (**Fig.2B**) and concentration against the intensity of the red, blue, green and total RGB (**Fig.3**). The light intensity of the color product were measured in safety cabinet with white interior, to obtain same environment and lighting condition for photography. The color product of AuNPs and codeine sulphate obtained was transferred in to micro centrifuge tubes and were photographed in this system with built in digital camera of the iPhone 5S which was set to "flash off" mode. In iPhone 5S backside illumination (BSI) CMOS image sensor was used which facilitate more incident light to reach the light sensing silicon. These properties allow the light to strike the photo cathode layer without passing through the wiring layer in the BSI CMOS sensor providing better sensitivity to detect small differences in photon emission from darker products as compared to any DSLR Camera[10a]. Each photographed image was saved as a JPEG (24-bits) on iPhone's memory, subsequently images were transferred to computer and opened in Adobe PhotoshopCS6. The fixed size box of 100 x 100 pixel was placed at fixed points on each micro centrifuge tube image with the help of Rectangular Marquee tool. The mean intensity of red, green and blue color of selected part was obtained by using the Histogram tool. This whole procedure was repeated five times and average of intensity of each were recorded in Excel (Version 2013) spreadsheet for data analysis (**Fig.1 (A)**).

The UV-Visible spectrum of the citrate capped AuNPs solution showed maximum absorption at 520 nm which remained same even after several months of storage. This indicates that microwave synthesized nanoparticles are stable. Citrate capped AuNPs are miscible with water and clear solution appears red. In our study, molecular-linker-based aggregation mechanism between AuNPs and codeine sulphate was monitored by UV-Vis spectrophotometer. During the study, various concentrations, 1 µM-50 µM, of drug solutions were treated with 0.07 mM AuNPs. Upon direct exposure of 0.1 mM codeine sulphate to citrate stabilized AuNPs, the solution immediately turned to purple color from wine red (**Fig.2**). This significant change in color indicates that citrate capped AuNPs recognize codeine sulphate. As shown in **Fig. S1** (**ESI**) the absorption ratio (A_{582}/A_{520}) remained unchanged after 2 min, indicating the interaction was almost completed under this condition. Therefore, all the absorption measurements were performed in 2 min. The surface plasmon absorption of citrate capped AuNPs solution were subjected to instantaneous exposure to increasing amounts of codeine sulphate from 7 µM to 1 µM as schemed in **Fig.2A**. With the addition of 0.1 mM codeine sulphate, the absorbance at 520 nm decreases dramatically and new band upturn at 582 nm, which confirms the

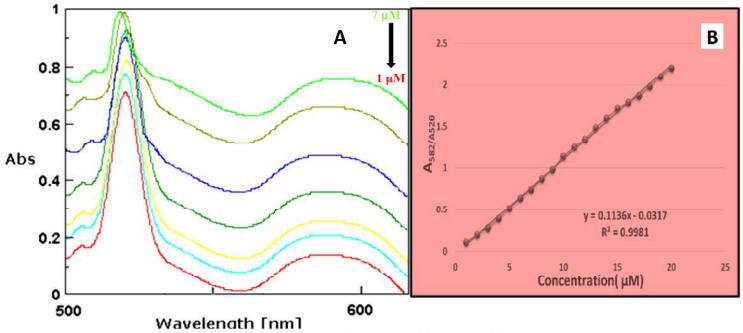

Fig.2 (**A**) UV-Visible spectra of solutions of 0.07 mM AuNPs responding to various concentrations of codeine sulphate. The curves from bottom to top shows gradually increasing concentrations of codeine sulphate: (a) 1 µM (b) 2 µM (c) 3 µM (d) 4 µM (e) 5 µM (f) 6 µM (g) 7 µM (**B**) Linear correlation with wide range of concentration (1-20 µM)of codeine sulphate with AuNPs

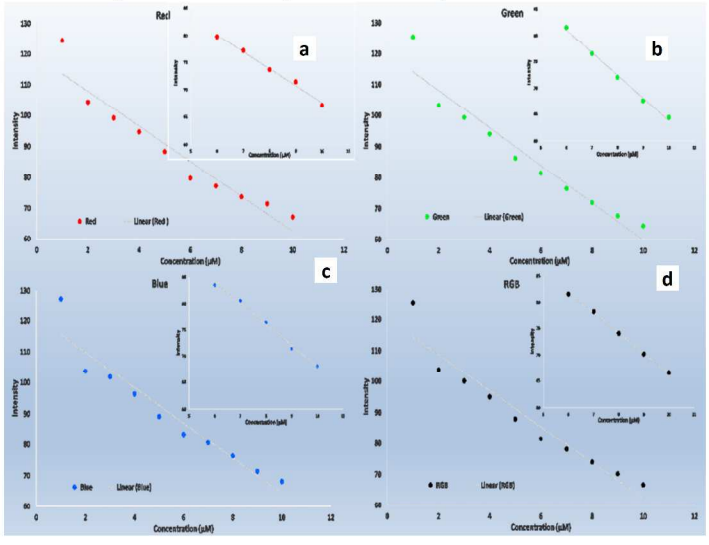

Fig.3 Relationship between (a) intensity of red light (b) intensity of green light (c) intensity of blue light (d) intensity of total RGB and codeine sulphate concentration (1 µM to 10 µM) from iPhone 5S images.

binding of codeine sulphate with AuNPs. **Fig. 2A** shows that, the intensity of new band rises with the increasing concentration of codeine sulphate. This indicates that more and more AuNPs were consumed to form more and more aggregates.

From the series of experiments, it was concluded that as the aggregation increases the size of the particles also increases which results in the color change. These changes in the intensity were noticed as a shift in UV Visible spectrogram. It is directly noticeable that there is a significant change in absorbance intensity at 520 nm to 582 nm upon increasing concentration of the codeine sulphate (**Fig.1B**). However, there is decrease in color intensity after 3 days due to sedimentation. The linear range for codeine sulphate, using 0.07 mM citrate capped AuNPs is found to be 1 μM - 20 μM (R^2 =0.998) (**Fig.2B**). The lower detection limit was found 0.9 μM (3σ) and shows fast response behaviour (<60 Sec) after addition of codeine sulphate into citrate stabilized AuNPs. The appearance of a new peak is due to the aggregation of AuNPs, which is caused by the replacement of citrate ions by codeine sulphate leading to the formation of AuNPs-cod complex (**Fig.1B**). This can be attributed to the greater electrostatic attraction of active groups of codeine sulphate with AuNPs than citrate groups, which is responsible for the additional band at longer wavelength. It has been shown theoretically and experimentally that aggregation of AuNPs leads to another plasmon absorption at longer wavelength when the individual nanoparticles are electronically coupled to each other. The oscillating electrons in one particle feel the electric field due to the oscillation of the free electrons in a second particle that can lead to a collective plasmonic oscillation of the aggregated system. This ligand exchange reaction or cross linking interaction provides an important means for the chemical functionalization of the nanoparticles and greatly extends the versatility of these systems. The relative absorbance change of AuNPs at 520 nm in the presence of 0.1 mM codeine sulphate and other drugs like, morphine, phenylephrine, phenobarbital, diazepam, lorazepam and clonazepam were measured to evaluate the selectivity of probe, where no such absorbance changes were observed (**Fig. S2, ESI**). The high selectivity of the codeine sulphate towards the nano probe may be due to the presence of three oxygen containing groups on one end binding to the citrate modified AuNPs and sulphate group (SO_3^{2-}) on the opposite end binding with the another citrate modified AuNPs, resulting in the aggregation.

The quantitative study of proposed nano probe with codeine sulphate was performed by smartphone. As discussed, the collected images opened in to Adobe PhotoshopCS6 software, automatically recognizes the color space of the picture. The R(ed), G(reen), and B(lue) intensities is representing the total photons in each region of the spectrum[15]. This phenomenon was used for the quantification in this study and results were found prominent (**Table S1, ESI)**. The range for codeine sulphate from 1 μM-10 μM were analyzed and were found to be linear. The graph shows that color intensities of the green and total RGB were more significant and gives good results (**Fig.3**). It was observed that blue and red light and codeine sulphate concentration was similar as both reflected by the color products. Both the color intensity showed good relationship between their intensity and codeine sulphate concentration (**Fig.3**).

Molecular linker-based aggregation of codeine sulphate conjugated AuNPs has been evaluated by dynamic light scattering (DLS) measurements which illustrated that the 0.07 mM AuNPs has an average hydrodynamic diameter of ~44 nm which maintain their size and stability (**Fig.4A**). Similarly, the addition of codeine sulphate solution (0.1 mM) to citrate stabilized AuNPs (0.07 mM), immediately resulted in aggregation and the size of nanoparticles increases to ~663 nm. The DLS histogram (**Fig.4B**) clearly confirms the cross linking between the codeine sulphate and citrate stabilized AuNPs. Upon addition of different codeine sulphate concentrations (1 μM, 10 μM), AuNPs agglomerated and the size increased to (~286 nm, ~413 nm) respectively (**Fig. S3, ESI**). Thus, AuNPs based DLS assay was able to show a response at a lower concentration of codeine sulphate with only smaller aggregates formation and at higher concentrations, codeine sulphate shows bigger aggregates. The cross linking based aggregation between codeine sulphate and citrate stabilized AuNPs is further confirmed by TEM. As shown in **Fig. 4C**, the TEM images of mono dispersed 0.07 mM AuNPs showed uniform particles with an average size of 44 nm

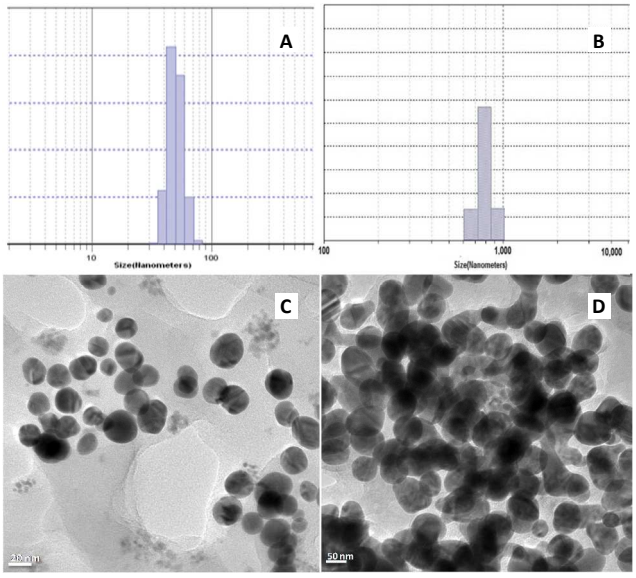

Fig.4. (A)DLS analysis of 0.07 mM AuNPs (**B**)after addition of 0.1 mM codeine sulphate to citrate capped AuNPs, **(C)** TEM micrograph of AuNPs and **(D)** after addition of 0.1 mM codeine sulphate into 0.07 mM AuNPs.

in diameter in the absence of codeine sulphate. However, after interaction with codeine sulphate, irregular AuNPs nanoaggregates were observed (**Fig.4D**). As mentioned earlier, this significantly indicates that citrate capped AuNPs will bind with codeine sulphate to form AuNPs–codeine sulphate nanoaggregates via cross linking interaction.

Ligand exchange reaction based AuNPs-cod complex is investigated by FT-IR spectroscopy. The FT-IR spectra of AuNPs and cod complex ranged between 4000–600 cm^{-1} with broad stretching vibrations of all characteristic functional moieties of ligands revealing their direct interaction with codeine sulphate. Vibrational spectra of codeine sulphate (**Fig S4A, ESI**) shows a broad band at 3415 cm^{-1}(-OH), 2923 cm^{-1}, 2831 cm^{-1} (asymmetric and symmetric -C–H stretching), and (C-N) 1143 cm^{-1}, (-S=O) 2599 cm^{-1} (SO_3^-) 1041 cm^{-1}, (O=S=O-stretching in SO_3H) 1378 cm^{-1}. Vibrational spectrum of AuNPs-cod complex is quite different as compared to codeine sulphate due to

disappearance of peak at (-S=O) 2599 cm^{-1} and shifting of peak at (C-N) 1196 cm^{-1}, (SO_3^-) 1081 cm^{-1}, (O=S=O-stretching in SO_3H) 1438 cm^{-1} (**Fig.S4 B, ESI**). As there was a very strong interlinked complex, it can be said that the peak difference is due to the ligand exchange reaction or electrostatic interaction.

Ligand exchange based complex formation between codeine sulphate and AuNPs are further confirmed by ESI-MS spectra. **Fig.S5 (ESI)** shows the ESI-MS spectra of the mixtures of codeine sulphate with AuNPs in aqueous solution, when the codeine sulphate was mixed with AuNPs in aqueous solution, where the molecular ion peak at m/z =893 was clearly detected, which undoubtedly suggests the formation of AuNPs-cod complex in the mixture.

The pH of the medium is another critical factor affecting the codeine sulphate detection. For the gold nanoprobe, the drug recognition became less efficient with pH elevation, so it was optimized at pH 6-9 and whole reactions were carried out on pH 7.5. The pH dependent of detection potently proves the aforementioned AuNPs-codeine ligand exchange or electrostatic interaction. Therefore, it is reasonable that the ligand exchange will be impeded greatly at higher pH condition (6.0-9.0) (**Fig S6, ESI**) as a consequence of the increase in the electrostatic interaction between codeine sulphate and citrate caped AuNPs. We also assessed the stability of citrate capped AuNPs assembly at different pH conditions (**Table S2, ESI**). It was perceived that AuNPs exhibited lower stability in solution of low pH ranging from 2 to 4 and were aggregated in few hours in the pH range of 7 to 10. The solution remained stable for weeks to months with no sign of further aggregation.

In order to evaluate the applicability and selectivity of the present assay, the determination of total drug content in bone, bone marrow and soil were performed using UV-Vis spectrophotometry (**ESI**). Extracted drug samples (**Scheme-1**) from bone, bone marrow and soil samples were initially diluted with deionised water as per the requirement, to fall into the linear range (1-50 μM), of our method and to obtain quantitative recovery of the treated samples. The total codeine sulphate content in bone, bone marrow and soil samples was also determined by the standard addition method. The control non treated real samples were also examined and compared. The recovery results ranged from 98% to 102.4%, indicating that no significant interference occurs in determination of drug from bone, bone marrow and soil samples after an appropriate dilution of the samples (**Table S3, ESI)**. The above results demonstrate that the drug mediated aggregation of AuNPs possesses great potential for detecting abused drug in post-mortem skeletal remains samples in forensic investigation.

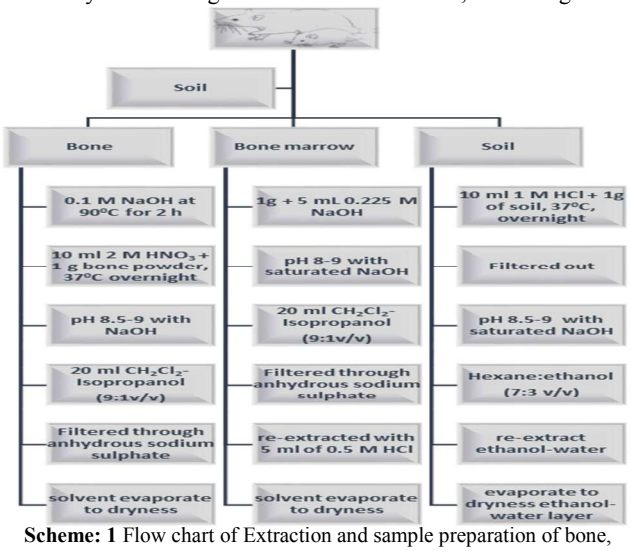

Scheme: 1 Flow chart of Extraction and sample preparation of bone, bone marrow and soil for codeine Sulphate

Conclusion

In summary, our proposed methods demonstrate that citrate capped gold nano probe, by formation of drug-nano complex, provides the potential to be used as an ideal novel platform for the development of a rapid, ultrasensitive, on site semi quantitative field test for the analysis of narcotics/codeine sulphate from post-mortem blood, skeletal remains and soil. Various correlations of the RGB value and the drug concentration were successfully established which explored a new paradigm for an application supporting a smart phone to be used as a primary analytical device, as to obtain an accurate concentration it is necessary to use a spectrophotometer and other higher instruments. Particularly attractive features of our probe are its simplicity, portability, economic viability and ability of on-spot detection of suspected drugs with the lower detection limit 0.9 μM (3σ) as compared to previous reported methods (**Table S4, ESI**)[18]. These advantages are likely to provide a wide and promising application of the easy, portable, cost effective and smart method for toxicological testing.

Acknowledgement

Financial support from UGC, New Delhi to one of the authors, Anand Lodha, is great fully acknowledged. The authors would like to acknowledge Dr. M. V. Rao (Head) and Mr. Rajendra, Department of Zoology, Gujarat University for their guidance and help.

References:

1. (a) M. A. Peat, *Cli. Lab. Med*. 1998, **2**, 263–278 (b) W. F. Smyth, M McClean, *Electrophoresis,* 1998, **19**, 2870-2882 (c) D. J. Crouch. *Forensic Sci. Int.* 2005, **150**, 165–173 (d) E. J. Cone, A. Zichterman, R. Heltsley, D. L. Black, B. Cawthon, T. Robert, F. Moser, Y. H. Caplan, *Forensic Sci. Int*. 2010, **198**, 58–61
2. (a) N. Raikos, H. Tsoukali, S. N. Njau, *Forensic Sci. Int*., 2001, **123** 140-141 (b) T. T. Noguchi, G. R. Nakamura, E. C. Griesemer. *J. Forensic Sci.* 1978, 23, **3**, 490–492 (c) J. H. Watterson and J. P. Donohue. *J. Anal. Tox*., 2011, 35,**7**, 452-458 (d) L. M. McIntyre, C. V. King, M. Boratto, O. H. Drummer. *Ther. Drug Moni..,* 2000, **22**,1, 79–83 (e) E. L. Horak, A.J. Jenkins, *J. Forensic Sci.* 2005, 50, **3**, 1–3 (f) K. K. McGrath, A. J. Jenkins. *Am. J. Forensic Med. Pathol.* 2009, 30,**1**, 40–44 (g) J. H. Watterson and J. E. Botman. *J. Forensic Sci.* 2009, **54**, 3, 708–714 (h)T. C. VandenBoer, S. A. Grummett, J. H. Watterson. *J. Forensic Sci.* 2008, **53**, 6, 1474–1482.
3. M. Freiermuth, J. C. Plasse, *J. Pharma. Biomed. Anal*, 1997, **15**, 759-764.
4. C. Moffat, M. D. Osselton, B. Widdop, *Clarke's Analysis of Drugs and Poisons in pharmaceuticals, body fluids and postmortem material*. Fourth Edition, Pharmaceutical Press, 2011.
5. B. Koleva, T. Kolev, R. Bakalska*, Spectrochimica. Acta. Part A* 2007, **67**, 196–201.
6. S. Popa, R. Oprean, E. Curea, N. Preda *J. Pharma. Biomed. Ana*l. 1998, **18**, 645–650.
7. Meadway, S. George, R. Braithwaite*, Forensic Sci. Int*., 2002, **127**, 136–141.
8. (a) L. Xiao, G. G. Wildgoose, R. G. Compton, *Anal. Chim. Acta*, 2008, **620**, 44-49 (b) H. Chi, B. Liu, G. Guan, Z. Zhang, M. Y. Han, *Analyst*, 2010, **135**, 1070–1075.
9. (a) S. J. Chen, Y. F. Huang, C. C. Huang, K. H. Lee, Z. H. Lin, H. T. Chang, *Biosens. Bioelectron*, 2008, **23**, 1749-1753 (b) M. S. Chen, D. W. Goodman, *Science*, 2004, **306**, 252-255 (c) C. W. Liu, Y. T. Hsieh, C. C. Huang, Z. H. Lin, H. T. Chang, *Chem. Commun*., 2008,

2242-2244 (d) K. L. Kelly, E. Coronado, L. L. Zhao, G. C. Schatz, *J. Phys. Chem. B*, 2003, **107**, 668-677 (e) C. C. Huang, Y. F. Huang, Z. Cao, W. H. Tan, H. T. Chang, *Anal. Chem*., 2005, **77**, 5735-5741

10. (a) A. Choodum, P. Kanatharana, W. Wongniramaikul, N. N. Daeid, *Talanta* 2013, **115**, 143–149 (b) N. Gaiao, V. L. Martins, W. d. S. Lyra, L. F. d. Almeida, E. C. d. Silva, M. C. U. Araujo, *Anal. Chim. Acta*. 2006, **570**, 283–290 (c) L. Byrne, J. Barker, G. Pennarun-Thomas, D. Diamond, S. Edwards, *Trends Analyt. Chem*. 2000, **19**, 517–522 (d) Lopez-Molinero, D. Linan, D. Sipiera, R. Falcon, *Microchem. J.* 2010, **96**, 380–385 (e) W. Silva Lyra, V. B. dosSantos, A. G. G. Dion3zio, V. L. Martins, L. F. Almeida, E. Nobrega Gaiao, P. H. G. D. Diniz, E. C. Silva, M. C. U. Araujo, *Talanta* 2009, **77**,1584–1589 (f) N. Maleki, A. Safavi, F. Sedaghatpour, *Talanta* 2004, **64**, 830–835 (g) Y. Suzuki, M.Endo, J. Jin, K. Iwase, M. Iwatsuki, *Anal. Sci*. 2006, **22**,411–414 (h) A. Choodum, N. NicDaeid, *Drug Test. Anal*. 2011, **3**, 277–282 (i) A. Choodum, N. NicDaeid, *Talanta*, 2011, **86**, 284–292 (j) A. Choodum, P. Kanatharana, W. Wongniramaikul, N. NicDaeid, *Forensic Sci. Int*. 2012, **222**, 340–345.
11. A. Pandya, H. Goswami, A. Lodha, S. K. Menon, *Analyst*, 2012, **137**, 1771-1774.
12. G. Patel, A. Kumar, U. Pal, S. Menon, *Chem. Commun*.2009, 1849–1851.
13. G. Patel, S. Menon, *Chem. Commun.* 2009, 3563–4356.
14. A. Lodha, A. Pandya, P. G. Sutariya, S. K. Menon, *Analyst*, 2013, **138**, 5411-5416.
15. A. Pandya, K. V. Joshi, N. R. Modi, S. K. Menon, *Sens. and Act.-B*, 2012, **168,** 54– 61.
16. (a)Z. Zhang, H. Sun, X. Shao, D. Li, H. Yu, M. Han, *Adv. Mater*., 2005, **17**, 42–47 (b) Z. Zhang, H. Yu, Y. Wang and M. Han, *Nanotechnology*, 2006, **17**, 2994–2997 (c) Z. Zhang, H. Yu, X. Shao, M. Han, *Chem.–Eur.* J., 2005, **11**, 3149–3154 (d) Yu, Z. Zhang, M. Han, X. Hao, F. Zhu, *J. Am. Chem. Soc*., 2005, **127**, 2378–2379 (e) G. Braun, I. Pavel, A. R. Morrill, D. S. Seferos, G. C. Bazan, N. O. Reich, M. Moskovits, *J. Am. Chem. Soc*., 2007, **129**,7760–7761 (f) M. Ji, W. Yang, Q. Ren, D. Lu, *Nanotechnology*, 2009, **20**, 075101, 11 (g) G. B. Braun, S. J. Lee, T. Laurence, N. Fera, L. Fabris, G. C. Bazan,M. Moskovits, N. O. Reich, *J. Phys. Chem. C,* 2009, **113**, 13622–13629 (h) Kundu, O. Neumann, B. G. Janesko, D. Zhang, S. Lal, A. Barhoumi, G. E. Scuseria, N. J. Halas, *J. Phys. Chem.* C, 2009, **113**, 14390–14397 (i) D. I. Gittins, F. Caruso, *Angew. Chem., Int. Ed*., 2001, **40**, 3001–3004.
17. (a) G Jiang , L. Wang , W. Chen, *Materials Letters*, 2007, **61**, 278–283 (b) N. T. K. Thanha, L. A. W. Greena, *Nano Today*, 2010 **5**, 213-230.
18. (a) L. Huanga, X. Yangb, C. Qib, X. Niua, C. Zhaoa, X. Zhaoa, D. Shangguanb,Y. Yanga, *Ana Chim Acta,* 2013, **787,** 203–210 (b) M. Saberian, H. Hamzeiy, A. Aghanejad, D. Asgari, 2011, BioImpacts**,** **1**(1), 31-36 (c) H. Touboua, A. Nameraa, Y. Arimaa, Y. Uchidab, A. Torikoshia, F. Moriyac, M. Nagaoa, *Legal Medicine*, 2014, DOI: 10.1016/j.legalmed.2014.04.004

Address:

[a]*Department of Forensic Science, School of Sciences, Gujarat University, Ahmedabad, Gujarat-380009, INDIA*
[b]*Institute of life sciences, Ahmedabad University, Ahmedabad, Gujarat-380009, INDIA*
[c]*Department of Chemistry, School of Sciences, Gujarat University, Ahmedabad, Gujarat-380009, INDIA*
E-mail:shobhanamenon07@gmail.com, forensicwithanand@gmail.com
Tel: +91-079-26300435.

gA smart and rapid colorimetric method for detection of codeine sulphate, using unmodified gold nanoprobe

Anand S. Lodha[a], Alok Pandya[b], Pinkesh Sutariya[c] and Shobhana K. Menon[ac]*

Graphical Abstract

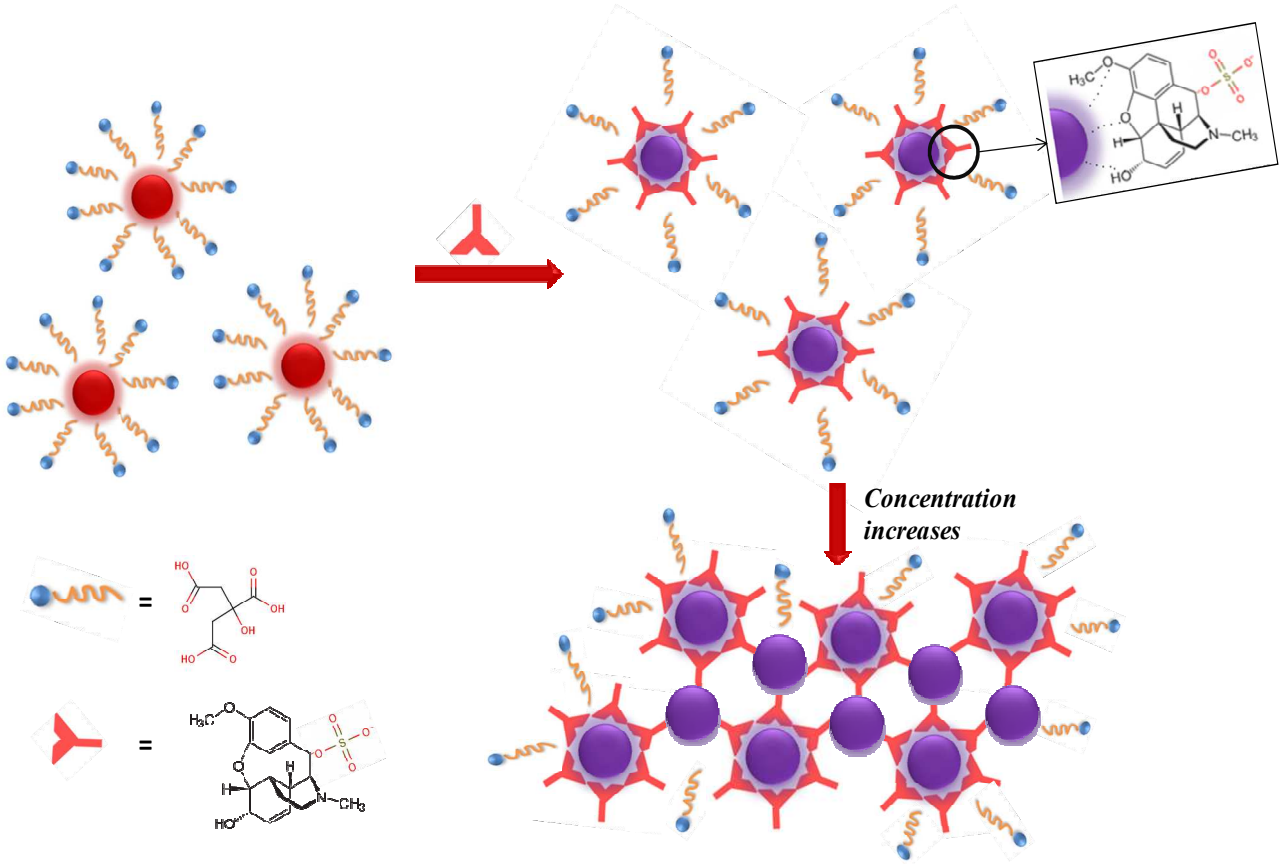

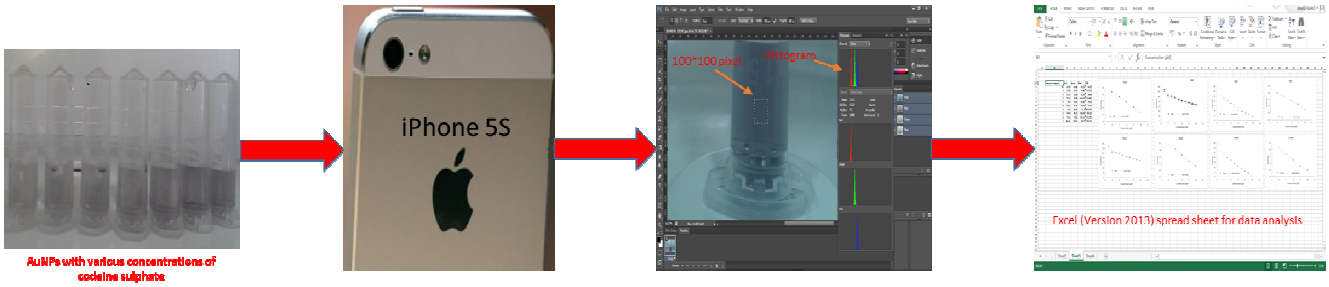

Herein, we reported unique optical and electrochemical properties of citrate stabilized gold Nanoparticles (AuNPs) as probe for smartphone assisted on spot detection of codeine sulphate in toxicological screening with high sensitivity (0.9 µM).